A Unique Liquefaction Case Study from the 29 May 2008, M_w6.3 Olfus Earthquake, Southwest Iceland

R.A. Green
Dept. of Civil and Environmental Engineering, Virginia Tech, Blacksburg, Virginia, USA

B. Halldorsson
Earthquake Engineering Research Centre, University of Iceland, Selfoss, Iceland

A. Kurtulus
Kandilli Observatory and Earthquake Research Institute, Bogazici University, Istanbul, Turkey

H. Steinarsson & O. Erlendsson
Dept. of Civil and Environmental Engineering, University of Iceland, Reykjavik, Iceland

SUMMARY:
The 2008, M_w6.3 Olfus earthquake induced liquefaction in volcanic sand deposits along the banks of an estuary located less than 1 km from the surface projection of the Kross fault rupture plane. This case history is unique because of the near-fault characteristics of the causative motions and because of the volcanic origin of the sands. In the study presented herein the authors compare the observed liquefaction response of the volcanic sand deposits to that predicted by the simplified liquefaction evaluation procedure. Although the procedure correctly predicts the occurrence of liquefaction, the severity of observed liquefaction was less than would be expected based on the low computed factors of safety. This is likely a consequence of the engineering properties of volcanic sand and may indicate the limited applicability of the simplified procedure for evaluating liquefaction potential of volcanic and other types of crushable sands. Also, it is possible that the factors of safety computed at the liquefaction sites are underestimated because of the short duration of the motions likely experienced at the sites.

Keywords: liquefaction, volcanic sands, Olfus earthquake, near-fault motions, Iceland

1. INTRODUCTION

In the study presented herein the authors compare the observed liquefaction response of the volcanic sand deposits during the 29 May 2008, M_w6.3 Olfus earthquake to that predicted by the simplified, stress-based liquefaction evaluation procedure. The primary objectives of this effort are to assess potential limitations of the simplified procedure for evaluating the liquefaction potential of volcanic sands and other types of crushable sands and to assess limitations in the procedure for evaluating the liquefaction potential in deposits subjected to near-fault motions. Iceland straddles the Mid-Atlantic Ridge, which is the diverging boundary between the North American and Eurasian tectonic plates. As such, Iceland is subjected to frequent earthquakes and volcanism. The largest earthquakes generally occur in the two transform zones shown in red in Fig. 1.1: the South Icelandic Seismic Zone (SISZ) in the south and the Tjornes Fracture Zone (TFZ) in the north (Halldorsson, 2009). In contrast, volcanism primarily occurs in the extensional zones, shown in tan in Fig. 1.1. Since the early 1700s, several damaging earthquakes have occurred in the SISZ ranging in magnitude from ~6 to ~7 (Welsh, 2009), with the latest being the 2008, M_w6.3 Olfus earthquake (Sigbjornsson et al., 2009). As its name implies, the Olfus earthquake occurred in the municipality of Olfus, which is in the westernmost part of the SISZ and is a relatively flat agricultural region with numerous small towns and villages. The earthquake resulted from slip on two adjacent, N-S trending, vertical, right lateral strike slip faults. As shown in Fig. 1.2, the initial slip occurred on the Ingolfsfjall fault about 4 km northeast of the town of Selfoss, followed ~2 seconds later by slip on the Kross fault, located about 4 km west of the Ingolfsfjall fault and running about 1 km east of the town of Hveragerdi (Hreinsdottir et al., 2009; Halldorsson et al., 2010).

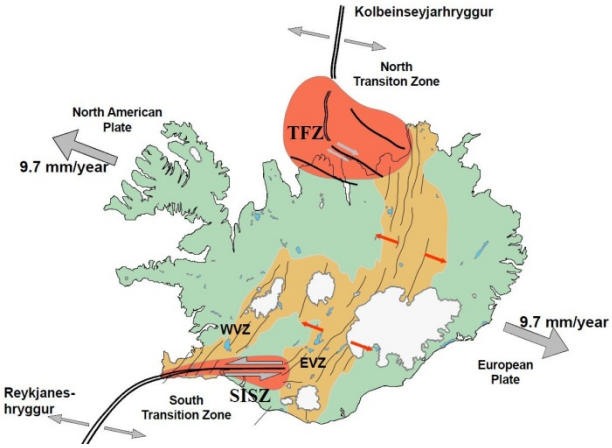

Figure 1.1. Tectonics of Iceland. (Halldorsson, 2009)

The Olfus earthquake damaged over 2000 buildings in Hveragerdi, Selfoss, and Eyrarbakki, with 24 buildings being damaged beyond economical repair (Sigbjornsson et al., 2009). Additionally, the earthquake induced liquefaction in volcanic sand deposits along the banks of an estuary of the River Olfusa located about 6.5 km south of Hveragerdi and less than 1 km from the surface projection of the nearest fault rupture plane (see Fig. 1.2). From a societal perspective, this occurrence of liquefaction was of little consequence. However, from an engineering perspective this liquefaction case study is unique because of the near fault characteristics of the causative motions and because of the volcanic origin of the sands. The most commonly used approach for evaluating liquefaction potential in engineering practice is the semi-empirical "simplified" procedure which is largely derived from earthquake liquefaction case histories of silica sand deposits (Whitman, 1971; Seed and Idriss, 1971; Youd et al., 2001). In contrast to silica sands, volcanic sand grains are more angular and crushable. Consequently, the engineering properties of these sands differ, and the applicability of the simplified procedure for evaluating liquefaction potential of volcanic sand deposits is unknown.

Figure 1.2. Satellite imagery of Olfus region annotated with the locations of the fault traces that ruptured during the 2008 Olfus earthquake and the volcanic sand deposits that liquefied.

2. GEOLOGY AND SOILS OF LIQUEFACTION SITES

As described by Atakan et al. (1997): *The bedrock geology of the SISZ was formed during the Upper Pliocene and Pleistocene (Saemundsson, 1979). The surface geology is dominated by young sequences (<0.7 Ma) of interbedded basaltic lavas and hyaloclastic breccias, which are intercalated with Quaternary sediments of mainly fluvial, glacial and glaciofulvial origin.* Specific to the study presented herein, the soils at the liquefaction sites are alluvial volcanic sand deposits of a few meters thick that lie along the banks of an estuary of the River Olfusa. These deposits are less than 1 km from the surface projection of the Kross fault rupture plane, which is the closer of the two faults that ruptured during the Olfus earthquake. Some of the sand boils that formed during this earthquake are shown in Fig. 2.1 (Sigval83, 2012; Jardvisindastofnun Haskolans, 2012). It is interesting to note that liquefaction also occurred along the banks of the River Olfusa during the Icelandic earthquakes of 1896 (Welsh, 2009; Thoroddsen, 1899). Two of the Olfus earthquake liquefaction sites were selected for detailed investigations, including dynamic cone penetration (DCP) in-situ tests and geotechnical laboratory soil characterization tests. The location of these sites lie within the region designated as "observed liquefaction" in Fig. 1.2, and the specific locations of these sites are shown in Fig. 2.2, designated as IPO1 and IPO4. One of the reasons for selecting these two sites was because their shear wave velocity profiles had previously been characterized (Bessason and Erlingsson, 2011).

(a) (b)

Figure 2.1. Sand boils that formed during the 2008 Olfus earthquake in a volcanic sand deposit along the banks of an estuary of the River Olfusa. (a. Sigval83, 2012; b. Jardvisindastofnun Haskolans, 2012)

Figure 2.2. Satellite imagery of volcanic sand deposits that liquefied during the 2008 Olfus earthquake annotated with the locations of DCP test sites.

Samples were collected from IPO1 and IPO4 using a hand auger, and laboratory tests were performed to determine the samples' grain size distribution, specific gravity, and minimum and maximum void ratios (or correspondingly, the minimum and maximum dry unit weights). The results of the tests are provided in Table 2.1 and Fig. 2.3. Interestingly, the specific gravity of the samples from the two sites differed fairly significantly, indicating different mineralogy and hence possibly different lava flows from which the sands weathered. Also, as may be observed from Fig. 2.3, the grain size distributions of the sands from the sites lie well within the boundaries identified by Tsuchida (1970) for "potentially liquefiable soils" and partially lie within the boundaries for "most liquefiable soils". Finally, photographs of the IPO1 and IPO4 samples from Scanning Electron Microscopy (SEM) analyses are shown in Fig. 2.4. Consistent with other volcanic sands, the grains shown in Fig. 2.4 are angular with some grains showing fractures.

Table 2.1. Engineering properties of volcanic sands at IPO1 and IPO4 liquefaction sites

	IPO1	IPO4
Specific Gravity, G_s	2.84	2.70
Coefficient of Uniformity, c_u	9	4.5
Coefficient of Gradation, c_z	1.21	0.98
USCS Classification	SW-SM	SP-SM
Fines Content, FC	7%	5.5%
maximum void ratio, e_{max}	1.40	1.67
minimum void ratio*, e_{min}	0.647-0.694	0.95-1.0
maximum dry unit weight*, γ_{dmax}	16.4-16.9 kN/m^3	13.2-13.6 kN/m^3
minimum dry unit weight, γ_{dmin}	11.6 kN/m^3	9.92 kN/m^3
γ_{sat} @ D_r = 35%	18.2 kN/m^3	16.7 kN/m^3

*e_{min} and γ_{dmax} were determined using ASTM standards for both the dry and wet methods

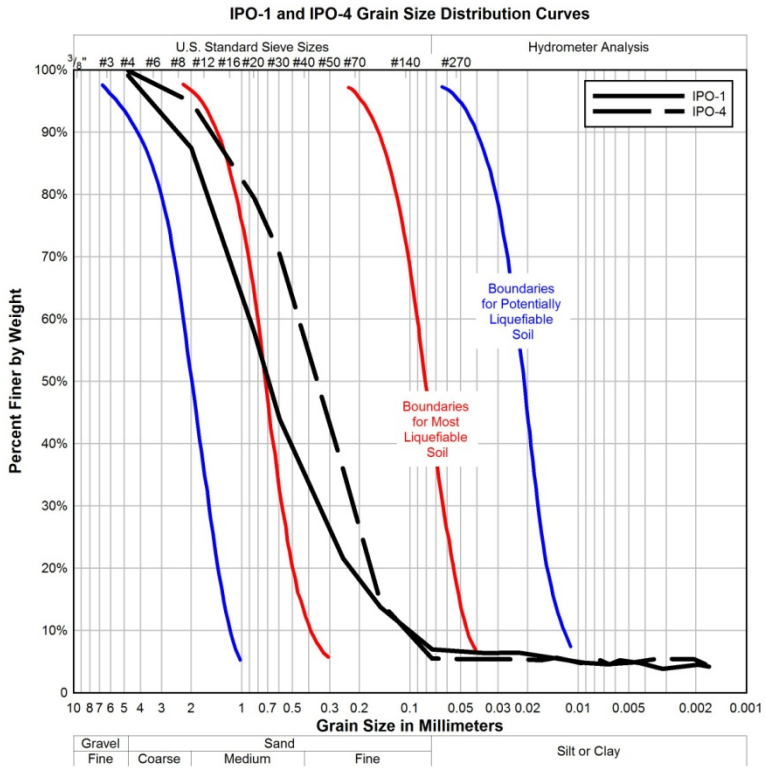

Figure 2.3. Grain size distribution curves of samples from IPO1 and IPO4. Also shown are the boundaries proposed by Tsuchida (1970) for "most liquefiable soil" and "potentially liquefiable soil".

3. IN-SITU TESTING

The in-situ tests were performed at IPO1 and IPO4 using the DCP designed by Sowers and Hedges (1966), with the DCP test shown being performed in Fig. 3.1. The Sowers and Hedges' DCP has been used on several other recent post-earthquake investigations to evaluate deposits that liquefied (e.g., the 2010, M_w7.0 Haiti earthquake, the 2010, M_w8.8 Maule, Chile earthquake, the 2010-2011 Canterbury, New Zealand earthquake sequence, and the 2011, M_w5.8 Central Virginia, USA earthquake). This system utilizes a 6.8 kg mass (15 lb weight) on an E-rod slide drive to penetrate an oversized 45° apex angle cone. The cone is oversized to reduce rod friction behind the tip. The DCP test consists of counting the number of drops of the mass that is required to advance the cone ~4.5 cm (1.75 inches), with the number of drops referred to as the DCP N-value or N_{DCPT}. There is an approximate one-to-one relationship between N_{DCPT} and SPT N-values up to about ~10 (Sowers and Hedges, 1966). However, beyond $N_{DCPT} \approx 10$, the relationship becomes non-linear with N_{DCPT} being greater than the corresponding SPT N-values. A slightly modified version the relationship between SPT and DCP N-values proposed by Sowers and Hedges (1966) was used in this study. The modifications to Sowers and Hedges (1966) relationship are based on tests performed by the first author (R. Green) in soils in the Canterbury region of New Zealand, where N_{DCPT} values were compared to SPT N-values, Cone Penetration Test (CPT) tip resistance, and shear wave velocity measurements made near the DCP test sites (Green et al., 2011).

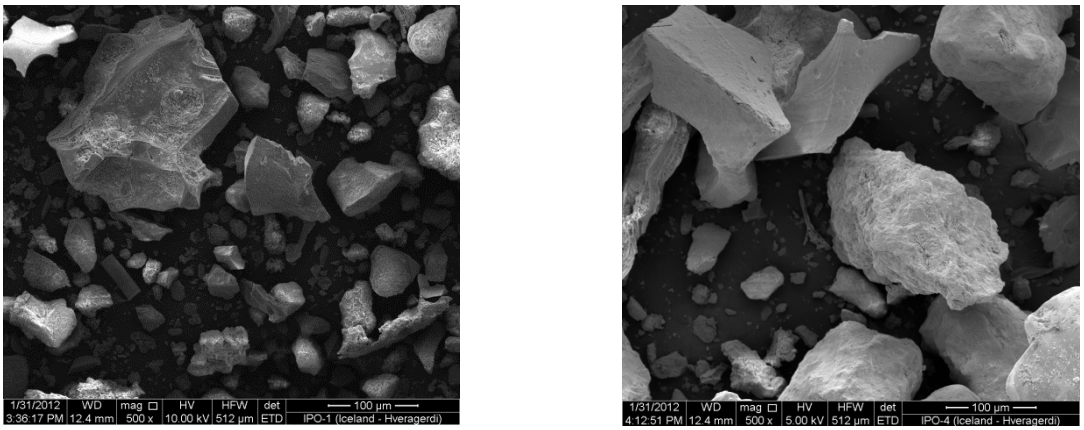

(a) (b)

Figure 2.4. Scanning Electron Microscopy photograph of volcanic sand samples: (a) IPO1 and (b) IPO4.

Following the procedure outlined in Olson et al. (2011), the SPT equivalent N-values ($N_{SPTequiv}$) values were normalized for effective overburden stress and hammer energy using the following relationship:

$$N_{1,60-SPT\ equiv} \approx N_{SPT\ equiv}(N_{DCPT}) \cdot \left(\frac{P_a}{\sigma'_{vo}}\right)^{0.5} \frac{ER}{60\%} \tag{3.1}$$

where $N_{SPTequiv}(N_{DCPT})$ is the functional relationship between N_{SPT} and N_{DCPT}, P_a is atmospheric pressure (i.e., 101.3 kPa), σ'_{vo} is initial vertical effective stress (in the same units as P_a), and ER is energy ratio. This relationship uses the effective stress and hammer energy normalization schemes outlined in Youd et al. (2001).

Although the energy ratio for the system was not measured, the DCP hammer is similar to the donut hammer used for the SPT. Skempton (1986) and Seed et al. (1984) suggested that the energy ratio for an SPT donut hammer system ranges from about 30 to 60%. However, because the DCP system does not have pulleys, a cathead, etc., we anticipate that the energy ratio for the DCP is likely to be near the upper end of this range. Therefore, we assumed an ER = 60% for our calculations. In addition to the effective stress and hammer energy corrections, the $N_{SPTequiv}$ values were also corrected for fines

content following the procedure proposed in Youd et al. (2001). Fig. 3.2 shows plots of N_{DCPT} and the computed equivalent $N_{1,60cs}$ for sites IPO1 and IPO4.

Figure 3.1. Performing a DCP test at IPO1.

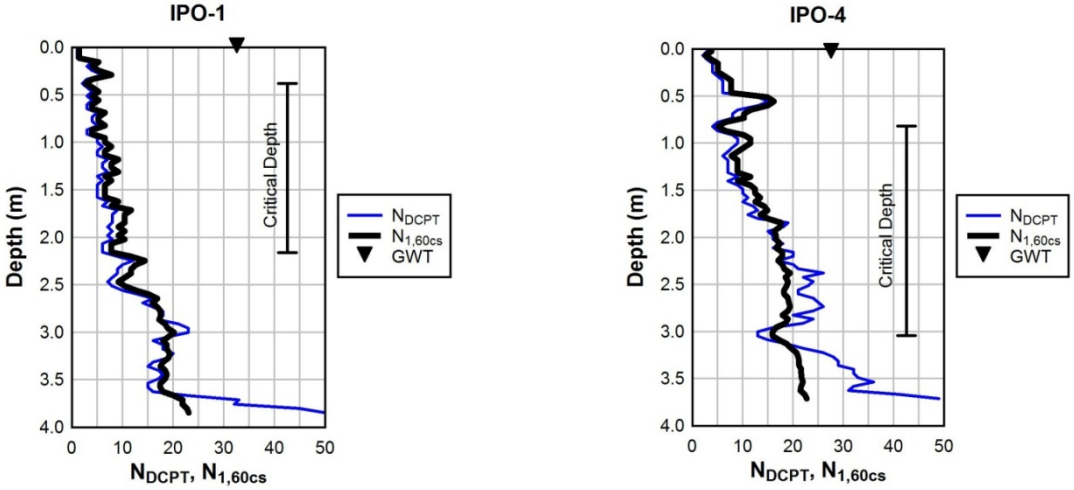

(a) (b)

Figure 3.2. Plot of N_{DCPT} and equivalent $N_{1,60cs}$ versus depth for: (a) IPO1 and (b) IPO4.

4. GROUND MOTIONS

As discussed in the next section, the in-situ test data described above correlates to the ability of the soil to resist liquefaction (i.e., capacity). However, to evaluate liquefaction potential, both the soil's ability to resist liquefaction and the demand imposed on the soil by the earthquake need to be known. For the approach used herein to evaluate liquefaction potential (i.e., stress-based simplified procedure), the amplitude of cyclic loading correlates to the geometric mean of the peak ground accelerations (a_{max}) of the two horizontal components at the ground surface, and the duration correlates to earthquake magnitude. Accordingly, the a_{max} at IPO1 and IPO4 needed to be estimated.

The earthquake motions from the Olfus event were well recorded by the small-aperture strong-motion array (ICEARRAY) in Hveragerdi and by the regional network of strong-motion stations (IceSMN). The motions recorded by the ICEARRAY are characterized by large horizontal peak ground accelerations ranging from 0.4 to 0.9g, pronounced velocity pulses in both the strike normal and strike parallel directions, and short strong-motion duration of 4 to 5 seconds (Halldorsson and Sigbjornsson, 2009). Note that the pronounced velocity pulses and short strong-motion durations are consistent with near-fault motions recorded in other earthquakes worldwide (e.g., Green et al., 2008). IPO1 and IPO4

have similar site-to-source distances as the seismographs comprising the ICEARRAY. Accordingly, it is assumed that the motions experienced at IPO1 and IPO4 were similar to those recorded by the ICEARRAY in Hveragerdi. Based on the geological/geotechnical site conditions, a_{max} at the IPO1 and IPO4 were estimated to be ~0.7g.

5. LIQUEFACTION EVALUATION

The simplified procedure (e.g., Whitman, 1971; Seed and Idriss, 1971) was used to evaluate liquefaction potential at IPO1 and IPO4. In its most basic form, the simplified procedure provides a factor of safety against liquefaction, with the demand imposed on the soil by the earthquake shaking expressed in terms of cyclic stress ratio (CSR) and the ability of the soil to resist liquefaction expressed in terms of cyclic resistance ratio (CRR). CSR is the ratio of the "average" shear stress induced in the soil column at a given depth, divided by the vertical effective stress at that same depth. However, because liquefaction is a fatigue-type phenomenon (Green and Terri, 2005), the duration of the earthquake motions needs to be taken into account, with the duration of shaking primarily being a function of earthquake magnitude. CSR was computed using the "simplified" equation (Youd et al., 2001):

$$CSR_{M\,7.5} = 0.65 \frac{a_{\max}}{g} \frac{\sigma_v}{\sigma'_{vo}} r_d \frac{1}{MSF} \tag{5.1}$$

where: $CSR_{M7.5}$ is the CSR adjusted to the duration of a magnitude 7.5 earthquake; a_{max} is the peak ground acceleration at the surface of the soil profile; σ_v is the total vertical stress at the depth of interest; σ'_{vo} is the vertical effective stress at the depth of interest; r_d is an empirically determined factor that is a function of depth and accounts for the reduction in CSR with depth; and MSF is a factor that accounts for the duration of the earthquake motions and is a function of earthquake magnitude. Assuming a_{max} = 0.7g, $CSR_{M7.5}$ at IPO1 and IPO4 were calculated using Eqn. 5.1, with r_d and average MSF obtained from Youd et al. (2001).

As outlined previously, equivalent SPT $N_{1,60cs}$ values were determined from the N_{DCPT} values using Eqn. 3.1. Once the $N_{1,60cs\text{-}SPTequiv}$ were determined, the following correlation proposed by Youd et al. (2001) was used to estimate the cyclic resistance ratio for a M_w7.5 event (i.e., $CRR_{M7.5}$):

$$CRR_{M\,7.5} = \frac{1}{34 - N_{1,60cs}} + \frac{N_{1,60cs}}{135} + \frac{50}{(10 \cdot N_{1,60cs} + 45)^2} - \frac{1}{200} \tag{5.2}$$

This relation is plotted in Fig. 5.1, and $CSR_{M7.5}$ and $CRR_{M7.5}$ are plotted as functions of depth in Fig. 5.2 for both IPO1 and IPO4.

As may be observed from Fig. 5.2, liquefaction is predicted to have occurred at both sites (i.e., $CSR_{M7.5} > CRR_{M7.5}$) over their entire depths. However, to further evaluate the liquefaction potential at IPO1 and IPO4, the DCP logs were analyzed and critical depths for liquefaction/thickness of the critical layers were selected. The thicknesses of the critical layers were selected based on trends in the N_{DCPT} values. As shown in Fig. 3.2 and 5.2, the thicknesses of the critical layers for IPO1 and IPO4 were ~1.75 m and ~2.25 m, respectively. Once the critical layers were determined for each test site, the $N_{1,60cs\text{-}SPTequiv}$ values, $CSR_{M7.5}$, and $CRR_{M7.5}$ were averaged over these depths. The results were plotted along with the $CRR_{M7.5}$ curve in Fig. 5.1. As with Fig. 5.2, both sites are predicted to have liquefied during the Olfus earthquake (i.e., the data points plot above the $CRR_{M7.5}$ curve).

6. DISCUSSION

As shown in Fig. 5.1 and 5.2, liquefaction was predicted using the simplified procedure to occur at both IPO1 and IPO4 during the Olfus earthquake, and indeed liquefaction occurred at these sites. However, given the relatively low factor of safety against liquefaction (FS) at these sites (i.e., FS = $CRR_{M7.5}/CSR_{M7.5}$) for the entire depths of the profiles, the authors would have expected the liquefaction to be much more severe than was evident by the relatively small sand boils observed (see Fig. 2.1). There may be a few reasons for this dichotomy. First, volcanic sand grains are much more crushable than silica sand grains. As a result, the N_{DCPT} values may represent the crushing strength of the volcanic sand grains more than the density of the sand deposits (and, hence, the intensity of shaking required to induce liquefaction). Also, as may be observed from Fig. 2.3, the volcanic sand particles are angular, and as such, likely have a tendency to dilate when sheared. This dilational tendency will have a mitigating effect on the formation of sand boils and the detrimental consequences of the initial triggering of liquefaction.

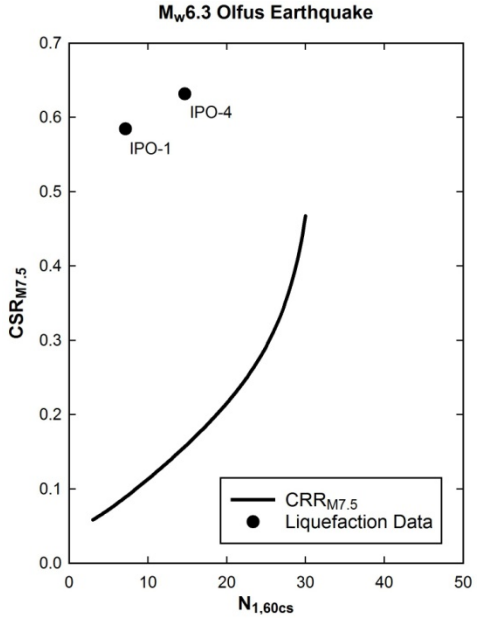

Figure 5.1. "Simplified" liquefaction evaluation chart with the data from IPO1 and IPO4 shown.

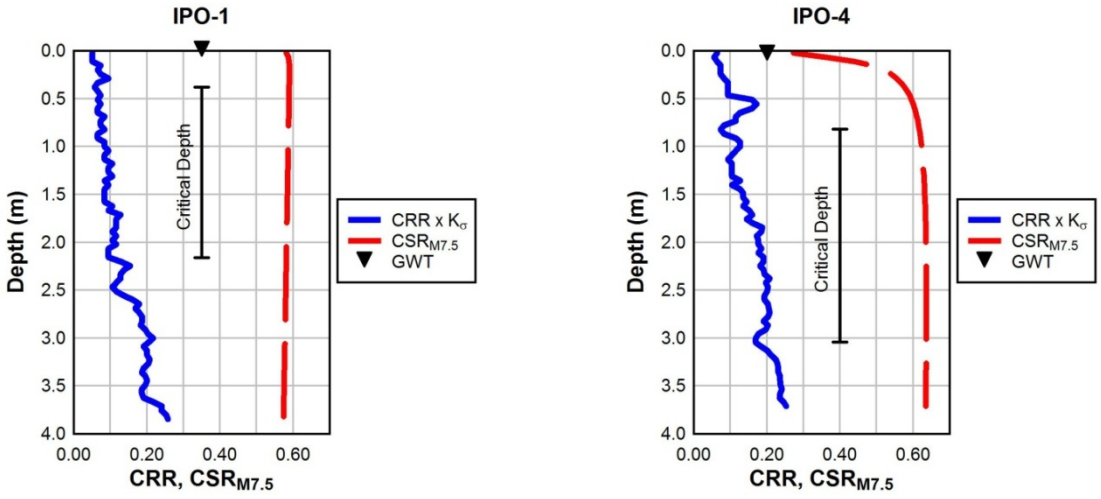

(a) (b)

Figure 5.2. Plot of $CRR_{M7.5}$ and $CSR_{M7.5}$ versus depth for: (a) IPO1 and (b) IPO4.

Another possible reason for the limited observed liquefaction is the relatively short duration of the ground motions. Because liquefaction is a fatigue phenomenon, both the amplitude and duration of the loading contribute to the demand imposed on the soil, with shorter durations imposing lesser demands. Per Eqn. 5.1, the duration is accounted for by the MSF, where duration and MSF are inversely related. For this study, the average of the range of MSF recommended by Youd et al. (2001) was used to compute $CSR_{M7.5}$. However, it has been well recognized that near-fault motions have shorter durations than "typical" motions (i.e., non near-fault motions). Accordingly, the MSF for near-fault motions would be expected to be greater than "typical" motions (Green et al., 2008). Thus, by using the MSF proposed by Youd et al. (2001) for typical motions, the computed $CSR_{M7.5}$, the $CSR_{M7.5}$ may have been over-estimated for IPO1 and IPO4 (or correspondingly, the FS at IPO1 and IPO4 may have been underestimated).

7. SUMMARY AND CONCLUSIONS

Although the simplified stress-based procedure correctly predicted the occurrence of liquefaction at the volcanic sand deposits analyzed, the severity of observed liquefaction was less than would be expected based on the low computed factors of safety. This is likely a consequence of the difference in the engineering properties of volcanic and silica sands, namely the crushability and dilative tendencies. As a result, these findings may indicate a limited applicability of the simplified procedure to evaluate the liquefaction potential of volcanic sand deposits (i.e., the simplified procedure may overestimate the liquefaction susceptibility of volcanic sands). Also, the deposits were subjected to near-fault motions, which characteristically have shorter strong motion durations than "typical" motions. Accordingly, the appropriateness of the MSF recommended by Youd et al. (2001) for evaluating liquefaction potential at sites subjected to near-fault motions needs further study. Finally, the readers are cautioned that these conclusions are preliminary and additional laboratory testing (i.e., cyclic triaxial and cyclic simple shear tests) is underway at Virginia Tech to better assess these initial findings.

ACKNOWLEDGEMENTS

The primary support for R. Green's participation in this study was provided by U.S. National Science Foundation (NSF) grants CMMI-0962952 and CMMI-1030564. This support is gratefully acknowledged. However, any opinions, findings, and conclusions or recommendations expressed in this material are those of the authors and do not necessarily reflect the views of the National Science Foundation. Also, the efforts of Mr. Kevin Foster, doctoral student at Virginia Tech, in performing the laboratory tests to characterize the volcanic sands are gratefully acknowledged.

REFERENCES

Atakan, K., Brandsdottir, B., Halldorsson, P. , and Fridleifsson, G.O. (1997). Site Response as a Function of Near-Surface Geology in the South Iceland Seismic Zone, *Natural Hazards*, **15**, 139-164.

Bessason, B. and Erlingsson, S. (2011). "Shear Wave Velocity in Surface Sediments", *Jokull*, Journal of the Glaciological and Geological Societies of Iceland, **61**, 51-64.

Green, R.A., Lee, J., White, T.M., and Baker, J.W. (2008). The Significance of Near-Fault Effects on Liquefaction, *Proc. 14th World Conf. on Earthquake Engineering*, Paper No. S26-019.

Green, R.A. and Terri, G.A. (2005). "Number of Equivalent Cycles Concept for Liquefaction Evaluations - Revisited", *Journal of Geotechnical and Geoenvironmental Engineering*, ASCE, **131:4**, 477-488.

Green, R.A., Wood, C., Cox, B., Cubrinovski, M., Wotherspoon, L., Bradley, B., Algie, T., Allen, J., Bradshaw, A., and Rix, G. (2011b). "Use of DCP and SASW Tests to Evaluate Liquefaction Potential: Predictions vs. Observations During the Recent New Zealand Earthquakes", *Seismological Research Letters*, **82:6**, 927-938.

Halldorsson, B. (2009). "ICEARRAY and the M6.3 Olfus earthquake on 29 May 2008 in South Iceland: Extreme near-fault strong-motion array recordings", *Proceedings of ISSEE2009*, University of Iceland, 29 May 2009.

Halldorsson, B. and Sigbjornsson, R. (2009). "The M_w6.3 Olfus Earthquake at 15:45 UTC on 29 May 2008 in

South Iceland: ICEARRAY Strong-Motion Recordings", *Soil Dynamics and Earthquake Engineering*, **29**, 1073-1083.

Halldorsson, B., Sigbjornsson, Chanerley, A.A., and Alexander, N.A. (2010). "Near-Fault Strong-Motion Array Recordings of the M_w6.3 Olfus Earthquake on 29 may 2008 in Iceland", *Proceedings of the 9th US National and 10th Canadian Conference on Earthquake Engineering*, Paper No. 1157.

Hreinsdottir, S., Arnadottir, T., Decriem, J., Geirsson, H., Tryggvason, A., Bennett, R.A., and LaFemina, P. (2009). "A Complex Earthquake Sequence Captured by the Continuous GPS Network in SW Iceland", *Geophysical Research Letters*, **36**, 5pgs.

Jardvisindastofnun Haskolans (2012). http://www.jardvis.hi.is/page/jh-skjalfti08

Olson, S.M., Green, R.A., Lasley, S., Martin, N., Cox, B.R., Rathje, E., Bachhuber, J., French, J. (2011). "Documenting Liquefaction and Lateral Spreading Triggered by the 12 January 2010 Haiti Earthquake", *Earthquake Spectra*, **27:S1**, S93-S116.

Saemundsson, K. (1979). Outline of the Geology of Iceland, *Jokul*, **29**, 7-28.

Seed, H.B. and Idriss, I.M. (1971) "Simplified procedure for evaluating soil liquefaction potential." *Journal of the Soil Mechanics and Foundations Division*, ASCE, **97:SM9**, 1249-1273.

Seed, H.B., K. Tokimatsu, L.F. Harder, and R. Chung (1984). The Influence of SPT Procedures on Soil Liquefaction Resistance Evaluations, Report No. UCB\EERC-84/15, Earthquake Engineering Research Center, Univ. California, Berkeley, CA.

Sigbjornsson, R., Snaebjornsson, J.T., Higgins, S.M., Halldorsson, B., and Olafsson, S. (2009). "A Note on the Mw 6.3 Earthquake in Iceland on 29 May 2008 at 15:45 UTC", *Bulletin of Earthquake Engineering*, **7**, 113-126.

Sigval83 (2012). http://sigval83.123.is/album/default.aspx?aid=99981

Skempton, A.W. (1986). Standard Penetration Test Procedures and the Effects in Sands of Overburden Pressure, Relative Density, Particle Size, Aging and Overconsolidation, *Geotechnique*, **36:3**, 425-447.

Sowers, G.F. and C.S. Hedges (1966) Dynamic cone for shallow in-situ penetration testing, vane shear and cone penetration resistance testing of in-situ soils. *ASTM STP 399, American Society of Testing Materials*, Philadelphia, PA, 29-37.

Thoroddsen, T. (1899). "Jardskjalftar a Sudurlandi", *Hid Islenska Bokmenntafjelag*, Kaupmannahofn, Iceland.

Tsuchida, H. (1970). Prediction and Countermeans Against the Liquefaction in Sand Deposits," *Abstracct of the Seminar in the Port and Harbor Research Institute*, Yokohama, Japan, 3.1-3.33.

Welsh, H.K. (2009). "Liquefaction Potential at a Proposed Hydroelectric Site in Iceland: Urridafoss Case Study Using Cone Penetration Data", Master's Thesis , Faculty of Civil and Environmental Engineering, University of Iceland, Reykjavic, Iceland, 97pgs.

Whitman, R.V. (1971). "Resistance of soil to liquefaction and settlements." *Soils and Foundations.* **11:4**, 59-68.

Youd, T.L., Idriss, I.M., Andrus, R.D., Arango, I., Castro, G.,Christian, J.T., Dobry, R., Finn, W.D.L., Harder, L.F., Hynes, M.E., Ishihara, K., Koester, J.P., Liao, S.C.S., Marcuson, W.F., Martin, G.R., Mitchell, J.K., Moriwaki, Y., Power, M.S., Robertson, P.K., Seed, R.B., and Stokoe, K.H. (2001) "Liquefaction resistance of soils: summary report from the 1996 and 1998 NCEER/NSF workshops on evaluation of liquefaction resistance of soils." *Journal of Geotechnical and Geoenvironmental Engineering.* ASCE, **127:10**, 817-833.